

2 **Omicron infection enhances neutralizing immunity against the Delta variant**

3 Khadija Khan^{1,2#}, Farina Karim^{1,2#}, Sandile Cele^{1,2}, James Emmanuel San³, Gila Lustig⁴, Houriiyah
4 Tegally^{3,5}, Mallory Bernstein¹, Yashica Ganga¹, Zesuliwe Jule¹, Kajal Reedy¹, Nokuthula Ngcobo¹,
5 Matilda Mazibuko¹, Ntombifuthi Mthabela¹, Zoey Mhlane¹, Nikiwe Mbatha¹, Jennifer Giandhari³,
6 Yajna Ramphal³, Taryn Naidoo¹, Nithendra Manickchand⁶, Nombulelo Magula⁷, Salim S. Abdool
7 Karim^{4,8}, Glenda Gray⁹, Willem Hanekom^{1,10}, Anne von Gottberg^{11,12}, , COMMIT-KZN Team[§],
8 Bernadett I. Gosnell⁶, Richard J. Lessells^{3,4}, Penny L. Moore^{4,11,12,13}, Tulio de Oliveira^{3,4,5,14}, Mahomed-
9 Yunus S. Moosa⁶, Alex Sigal^{1,2,15*}

10 ¹Africa Health Research Institute, Durban, South Africa. ²School of Laboratory Medicine and Medical
11 Sciences, University of KwaZulu-Natal, Durban, South Africa. ³KwaZulu-Natal Research Innovation
12 and Sequencing Platform, Durban, South Africa. ⁴Centre for the AIDS Programme of Research in
13 South Africa, Durban, South Africa. ⁵Centre for Epidemic Response and Innovation, School of Data
14 Science and Computational Thinking, Stellenbosch University, Stellenbosch, South Africa.
15 ⁶Department of Infectious Diseases, Nelson R. Mandela School of Clinical Medicine, University of
16 KwaZulu-Natal, Durban, South Africa. ⁷Department of Internal Medicine, Nelson R. Mandela School
17 of Medicine. University of Kwa-Zulu Natal. ⁸Department of Epidemiology, Mailman School of Public
18 Health, Columbia University, New York, NY, United States. ⁹South African Medical Research Council,
19 Cape Town, South Africa. ¹⁰Division of Infection and Immunity, University College London, London,
20 UK. ¹¹National Institute for Communicable Diseases of the National Health Laboratory Service,
21 Johannesburg, South Africa. ¹²SAMRC Antibody Immunity Research Unit, School of Pathology, Faculty
22 of Health Sciences, University of the Witwatersrand, Johannesburg, South Africa. ¹³Institute of
23 Infectious Disease and Molecular Medicine, University of Cape Town, Cape Town, South Africa.
24 ¹⁴Department of Global Health, University of Washington, Seattle, USA. ¹⁵Max Planck Institute for
25 Infection Biology, Berlin, Germany.

26 * Corresponding author. Email: alex.sigal@ahri.org

27

28 **Omicron has been shown to be highly transmissible and have extensive evasion of neutralizing**
29 **antibody immunity elicited by vaccination and previous SARS-CoV-2 infection. Omicron infections**
30 **are rapidly expanding worldwide often in the face of high levels of Delta infections. Here we**
31 **characterized developing immunity to Omicron and investigated whether neutralizing immunity**
32 **elicited by Omicron also enhances neutralizing immunity of the Delta variant. We enrolled both**
33 **previously vaccinated and unvaccinated individuals who were infected with SARS-CoV-2 in the**
34 **Omicron infection wave in South Africa soon after symptom onset. We then measured their ability**
35 **to neutralize both Omicron and Delta virus at enrollment versus a median of 14 days after**
36 **enrollment. Neutralization of Omicron increased 14-fold over this time, showing a developing**
37 **antibody response to the variant. Importantly, there was an enhancement of Delta virus**
38 **neutralization, which increased 4.4-fold. The increase in Delta variant neutralization in individuals**
39 **infected with Omicron may result in decreased ability of Delta to re-infect those individuals. Along**
40 **with emerging data indicating that Omicron, at this time in the pandemic, is less pathogenic than**
41 **Delta, such an outcome may have positive implications in terms of decreasing the Covid-19 burden**
42 **of severe disease.**

43

44 The Omicron variant of SARS-CoV-2, first identified in November 2021 in South Africa and Botswana,
45 has been shown by us¹ and others²⁻⁷ to have extensive but incomplete escape from immunity elicited
46 by vaccines and previous infection, with boosted individuals showing effective neutralization, even
47 though vaccine and booster efficacy may wane over time.

NOTE: This preprint reports new research that has not been certified by peer review and should not be used to guide clinical practice.

48 (https://assets.publishing.service.gov.uk/government/uploads/system/uploads/attachment_data/file/1043807/technical-briefing-33.pdf). In South Africa Omicron infections led to a lower incidence of
49 severe disease relative to other variants⁸, although this can be at least partly explained by pre-existing
50 immunity¹. While Omicron infections are rising steeply, many countries still have high levels of
51 infection with the Delta variant. How Delta and Omicron will interact is still unclear, and one possibility
52 is that Omicron will curtail the spread of Delta by eliciting a neutralizing immune response against
53 Delta in people infected by Omicron.
54

55 We investigated whether Omicron infection elicits neutralizing immunity to the Delta variant. We
56 isolated Omicron virus without the R346K mutation from an infection in South Africa. This virus had
57 similar neutralization escape (Fig S1) as a previous Omicron isolate with the R346K mutation¹. We
58 neutralized this isolate with plasma from the blood of 15 participants enrolled during the Omicron
59 infection wave in South Africa, with each participant having a confirmed diagnosis of SARS-CoV-2 by
60 qPCR. To quantify neutralization, we used a live virus neutralization assay and calculated the focus
61 reduction neutralization test (FRNT₅₀) value, the inverse of the plasma dilution required for 50%
62 reduction in infection foci. The majority infecting viruses from the enrolled participants were
63 successfully sequenced and all of these were Omicron (Table S1).

64 Eleven out of 15 participants were admitted to hospital because of Covid-19 symptoms, but none
65 required supplemental oxygen. Participants were sampled at enrollment, which was a median of 4
66 days post-symptom onset and again at a median of 14 days post-enrollment. Two participants did not
67 detectably neutralize Omicron at either timepoint and were excluded from the analysis. Two of the
68 remaining 13 participants did not have detectable SARS-CoV-2 at enrollment, indicating that infection
69 was already cleared, and therefore that these participants were sampled later post-infection. Out of
70 the 13 participants, 7 were vaccinated, 3 with two doses of Pfizer-BNT162b2 and 4 with Johnson and
71 Johnson Ad26.CoV2.S (Table S1) with one of the Ad26.CoV2.S vaccines being boosted with a second
72 Ad26.CoV2.S dose.

73 We measured neutralization at enrollment and the later visit and observed that Omicron
74 neutralization increased from a low geometric mean (GMT) FRNT₅₀ of 20 to 285, a 14.4-fold increase
75 (95% CI 5.5-37.4, Fig 1A). Importantly, neutralization of Delta increased during this period 4.4-fold
76 (95% CI 2.1-9.2), from FRNT₅₀ of 80 to 354 (Fig 1B). The two participants who were likely sampled at a
77 longer time post-infection showed relatively high neutralization values at enrollment both against
78 Omicron and Delta virus, and these did not appreciably increase with time, indicating that
79 neutralization capacity plateaued before enrollment. Comparing Omicron and Delta neutralization at
80 the last available timepoint showed that vaccinated participants were able to mount a better
81 neutralizing response against Delta virus, while the response in unvaccinated participants was more
82 variable (Fig 1C).

83 The ability of one variant to elicit immunity which can cross-neutralize another variant varies by
84 variant⁹⁻¹¹. Immunity elicited by Delta infection does not cross-neutralize Beta virus and Beta elicited
85 immunity does not cross-neutralize Delta well^{12,13}. However, participants in this study have likely been
86 previously infected, and more than half were vaccinated. Therefore, it is unclear if what we observe
87 is effective cross-neutralization of Delta virus by Omicron elicited antibodies, or activation of antibody
88 immunity from previous infection and/or vaccination.

89 These results are consistent with Omicron displacing the Delta variant, since it can elicit immunity
90 which neutralizes Delta making re-infection with Delta less likely. In contrast, Omicron escapes
91 neutralizing immunity elicited by Delta⁶ and therefore may re-infect Delta infected individuals. The
92 implications of such displacement would depend on whether Omicron is indeed less pathogenic than
93 Delta. If so, then the incidence of Covid-19 severe disease would be reduced and the infection may
94 shift to become less disruptive to individuals and society.

95

96 **Materials and methods**

97 Informed consent and ethical statement

98 Blood samples were obtained after written informed consent from adults with PCR-confirmed SARS-
99 CoV-2 infection who were enrolled in a prospective cohort study approved by the Biomedical Research
100 Ethics Committee at the University of KwaZulu-Natal (reference BREC/00001275/2020). Use of
101 residual swab sample was approved by the University of the Witwatersrand Human Research Ethics
102 Committee (HREC) (ref. M210752).

103 Data availability statement

104 Sequence of outgrown virus has been deposited in GISAID with accession EPI_ISL_7886688. Raw
105 images of the data are available upon reasonable request.

106 Code availability

107 Image analysis and curve fitting scripts in MATLAB v.2019b are available on GitHub
108 (<https://github.com/sigallab/NatureMarch2021>).

109 Whole-genome sequencing, genome assembly and phylogenetic analysis

110 RNA was extracted on an automated Chemagic 360 instrument, using the CMG-1049 kit (Perkin Elmer,
111 Hamburg, Germany). The RNA was stored at -80°C prior to use. Libraries for whole genome
112 sequencing were prepared using either the Oxford Nanopore Midnight protocol with Rapid Barcoding
113 or the Illumina COVIDseq Assay. For the Illumina COVIDseq assay, the libraries were prepared
114 according to the manufacturer's protocol. Briefly, amplicons were tagmented, followed by indexing
115 using the Nextera UD Indexes Set A. Sequencing libraries were pooled, normalized to 4 nM and
116 denatured with 0.2 N sodium acetate. A 8 pM sample library was spiked with 1% PhiX (PhiX Control
117 v3 adaptor-ligated library used as a control). We sequenced libraries on a 500-cycle v2 MiSeq Reagent
118 Kit on the Illumina MiSeq instrument (Illumina). On the Illumina NextSeq 550 instrument, sequencing
119 was performed using the Illumina COVIDSeq protocol (Illumina Inc, USA), an amplicon-based next-
120 generation sequencing approach. The first strand synthesis was carried using random hexamers
121 primers from Illumina and the synthesized cDNA underwent two separate multiplex PCR reactions.
122 The pooled PCR amplified products were processed for tagmentation and adapter ligation using IDT
123 for Illumina Nextera UD Indexes. Further enrichment and cleanup was performed as per protocols
124 provided by the manufacturer (Illumina Inc). Pooled samples were quantified using Qubit 3.0 or 4.0
125 fluorometer (Invitrogen Inc.) using the Qubit dsDNA High Sensitivity assay according to manufacturer's
126 instructions. The fragment sizes were analyzed using TapeStation 4200 (Invitrogen). The pooled
127 libraries were further normalized to 4nM concentration and 25 μL of each normalized pool containing
128 unique index adapter sets were combined in a new tube. The final library pool was denatured and
129 neutralized with 0.2N sodium hydroxide and 200 mM Tris-HCL (pH7), respectively. 1.5 pM sample
130 library was spiked with 2% PhiX. Libraries were loaded onto a 300-cycle NextSeq 500/550 HighOutput
131 Kit v2 and run on the Illumina NextSeq 550 instrument (Illumina, San Diego, CA, USA). For Oxford
132 Nanopore sequencing, the Midnight primer kit was used as described by Freed and Silander55. cDNA
133 synthesis was performed on the extracted RNA using LunaScript RT mastermix (New England BioLabs)
134 followed by gene-specific multiplex PCR using the Midnight Primer pools which produce 1200bp
135 amplicons which overlap to cover the 30-kb SARS-CoV-2 genome. Amplicons from each pool were
136 pooled and used neat for barcoding with the Oxford Nanopore Rapid Barcoding kit as per the
137 manufacturer's protocol. Barcoded samples were pooled and bead-purified. After the bead clean-up,
138 the library was loaded on a prepared R9.4.1 flow-cell. A GridION X5 or MinION sequencing run was
139 initiated using MinKNOW software with the base-call setting switched off. We assembled paired-end

140 and nanopore.fastq reads using Genome Detective 1.132 (<https://www.genomedetective.com>) which
141 was updated for the accurate assembly and variant calling of tiled primer amplicon Illumina or Oxford
142 Nanopore reads, and the Coronavirus Typing Tool⁵⁶. For Illumina assembly, GATK HaploTypeCaller --
143 min-pruning 0 argument was added to increase mutation calling sensitivity near sequencing gaps. For
144 Nanopore, low coverage regions with poor alignment quality (<85% variant homogeneity) near
145 sequencing/amplicon ends were masked to be robust against primer drop-out experienced in the
146 Spike gene, and the sensitivity for detecting short inserts using a region-local global alignment of
147 reads, was increased. In addition, we also used the wf_artic (ARTIC SARS-CoV-2) pipeline as built using
148 the nextflow workflow framework⁵⁷. In some instances, mutations were confirmed visually with .bam
149 files using Geneious software V2020.1.2 (Biomatters). The reference genome used throughout the
150 assembly process was NC_045512.2 (numbering equivalent to MN908947.3). For lineage
151 classification, we used the widespread dynamic lineage classification method from the 'Phylogenetic
152 Assignment of Named Global Outbreak Lineages' (PANGOLIN) software suite
153 (<https://github.com/hCoV-2019/pangolin>)¹⁹. P2 stock was sequenced and confirmed Omicron with
154 the following substitutions:
155 E:T9I,M:D3G,M:Q19E,M:A63T,N:P13L,N:R203K,N:G204R,ORF1a:K856R,ORF1a:L2084I,ORF1a:A2710T,
156 ORF1a:T3255I,ORF1a:P3395H,ORF1a:I3758V,ORF1b:P314L,ORF1b:I1566V,ORF9b:P10S,S:A67V,S:T95I
157 ,S:Y145D,S:L212I,S:G339D,S:S371L,S:S373P,S:S375F,S:K417N,S:N440K,S:G446S,S:S477N,S:T478K,S:E4
158 84A,S:Q493R,S:G496S,S:Q498R,S:N501Y,S:Y505H,S:T547K,S:D614G,S:H655Y,S:N679K,S:P681H,S:N76
159 4K,S:D796Y,S:N856K,S:Q954H,S:N969K,S:L981F. Sequence was deposited in GISAID, accession:
160 EPI_ISL_7886688.

161 Cells

162 Vero E6 cells (ATCC CRL-1586, obtained from Cellonex in South Africa) were propagated in complete
163 growth medium consisting of Dulbecco's Modified Eagle Medium (DMEM) with 10% fetal bovine
164 serum (Hyclone) containing 10mM of HEPES, 1mM sodium pyruvate, 2mM L-glutamine and 0.1mM
165 nonessential amino acids (Sigma-Aldrich). Vero E6 cells were passaged every 3–4 days. H1299 cell lines
166 were propagated in growth medium consisting of complete Roswell Park Memorial Institute (RPMI)
167 1640 medium with 10% fetal bovine serum containing 10mM of HEPES, 1mM sodium pyruvate, 2mM
168 L-glutamine and 0.1mM nonessential amino acids. H1299 cells were passaged every second day. The
169 H1299-E3 (H1299-ACE2, clone E3) cell line was derived from H1299 (CRL-5803) as described in our
170 previous work⁹ and Figure S1. Briefly, vesicular stomatitis virus G glycoprotein (VSVG) pseudotyped
171 lentivirus containing hACE2 was used to spinfect H1299 cells. ACE-2 transduced H1299 cells
172 (containing an endogenously yellow fluorescent protein labelled histone H2AZ gene¹⁴) were then
173 subcloned at the single cell density in 96-well plates (Eppendorf) in conditioned media derived from
174 confluent cells. After 3 weeks, wells were detached using a 0.25% trypsin-EDTA solution (Gibco) and
175 plated in two replicate plates, where the first plate was used to determine infectivity and the second
176 was stock. The first plate was screened for the fraction of mCherry positive cells per cell clone upon
177 infection with a SARS-CoV-2 mCherry expressing spike pseudotyped lentiviral vector. Screening was
178 performed using a Metamorph-controlled (Molecular Devices, Sunnyvale, CA) Nikon TiE motorized
179 microscope (Nikon Corporation, Tokyo, Japan) with a 20x, 0.75 NA phase objective, 561 nm laser line,
180 and 607 nm emission filter (Semrock, Rochester, NY). Images were captured using an 888 EMCCD
181 camera (Andor). The clone with the highest fraction of mCherry expression was expanded from the
182 stock plate and denoted H1299-E3. Infectivity was confirmed with mCherry expressing lentivirus by
183 flow cytometry using a BD Fortessa instrument and analyzed using BD FACSDiva Software (BD
184 Biosciences). This clone was used in the outgrowth and focus forming assay. Cell lines have not been
185 authenticated. The cell lines have been tested for mycoplasma contamination and are mycoplasma
186 negative.

187

188 Virus expansion

189 All work with live virus was performed in Biosafety Level 3 containment using protocols for SARS-CoV-
190 2 approved by the Africa Health Research Institute Biosafety Committee. ACE2-expressing H1299-E3
191 cells were seeded at 4.5×10^5 cells in a 6 well plate well and incubated for 18–20 h. After one DPBS
192 wash, the sub-confluent cell monolayer was inoculated with 500 μ L universal transport medium
193 diluted 1:1 with growth medium filtered through a 0.45- μ m filter. Cells were incubated for 1 h. Wells
194 were then filled with 3 mL complete growth medium. After 4 days of infection (completion of passage
195 1 (P1)), cells were trypsinized, centrifuged at 300 rcf for 3 min and resuspended in 4 mL growth
196 medium. Then all infected cells were added to Vero E6 cells that had been seeded at 2×10^5 cells per
197 mL, 20mL total, 18–20 h earlier in a T75 flask for cell-to-cell infection. The coculture of ACE2-expressing
198 H1299-E3 and Vero E6 cells was incubated for 1 h and the flask was then filled with 20 mL of complete
199 growth medium and incubated for 4 days. The viral supernatant (passage 2 (P2) stock) was used for
200 experiments.

201 Live virus neutralization assay

202 H1299-E3 cells were plated in a 96-well plate (Corning) at 30,000 cells per well 1 day pre-infection.
203 Plasma was separated from EDTA-anticoagulated blood by centrifugation at 500 rcf for 10 min and
204 stored at -80°C . Aliquots of plasma samples were heat-inactivated at 56°C for 30 min and clarified by
205 centrifugation at 10,000 rcf for 5 min. Virus stocks were used at approximately 50-100 focus-forming
206 units per microwell and added to diluted plasma. Antibody–virus mixtures were incubated for 1 h at
207 37°C , 5% CO_2 . Cells were infected with 100 μ L of the virus–antibody mixtures for 1 h, then 100 μ L of
208 a 1X RPMI 1640 (Sigma-Aldrich, R6504), 1.5% carboxymethylcellulose (Sigma-Aldrich, C4888) overlay
209 was added without removing the inoculum. Cells were fixed 18 h post-infection using 4% PFA (Sigma-
210 Aldrich) for 20 min. Foci were stained with a rabbit anti-spike monoclonal antibody (BS-R2B12,
211 GenScript A02058) at 0.5 $\mu\text{g}/\text{mL}$ in a permeabilization buffer containing 0.1% saponin (Sigma-Aldrich),
212 0.1% BSA (Sigma-Aldrich) and 0.05% Tween-20 (Sigma-Aldrich) in PBS. Plates were incubated with
213 primary antibody overnight at 4°C , then washed with wash buffer containing 0.05% Tween-20 in PBS.
214 Secondary goat anti-rabbit HRP conjugated antibody (Abcam ab205718) was added at 1 $\mu\text{g}/\text{mL}$ and
215 incubated for 2 h at room temperature with shaking. TrueBlue peroxidase substrate (SeraCare 5510-
216 0030) was then added at 50 μ L per well and incubated for 20 min at room temperature. Plates were
217 imaged in an ImmunoSpot Ultra-V S6-02-6140 Analyzer ELISPOT instrument with BioSpot Professional
218 built-in image analysis (C.T.L).

219 Statistics and fitting

220 All statistics and fitting were performed using custom code in MATLAB v.2019b. Neutralization data
221 were fit to:

$$222 \quad T_x = 1 / (1 + (D / ID_{50}))$$

223 Here T_x is the number of foci normalized to the number of foci in the absence of plasma on the same
224 plate at dilution D and ID_{50} is the plasma dilution giving 50% neutralization. $FRNT_{50} = 1 / ID_{50}$. Values of
225 $FRNT_{50} < 1$ are set to 1 (undiluted), the lowest measurable value. We note that the most concentrated
226 plasma dilution was 1:25 and therefore $FRNT_{50} < 25$ were extrapolated. We have marked these values
227 in Figure 1C and calculate the fold-change $FRNT_{50}$ either for the raw values or for values where $FRNT_{50}$
228 > 25 in Figure 1D.

229 Acknowledgements

230 This study was supported by the Bill and Melinda Gates award INV-018944 (AS), National Institutes of
231 Health award R01 AI138546 (AS), and South African Medical Research Council awards (AS, TdO, PLM)
232 and the UK Foreign, Commonwealth and Development Office and Wellcome Trust (Grant no
233 221003/Z/20/Z, PLM). PLM is also supported by the South African Research Chairs Initiative of the

234 Department of Science and Innovation and the NRF (Grant No 98341). The funders had no role in study
235 design, data collection and analysis, decision to publish, or preparation of the manuscript.

236 References

- 237 1 Cele, S. *et al.* Omicron extensively but incompletely escapes Pfizer BNT162b2 neutralization.
238 *Nature*, doi:doi: <https://doi.org/10.1038/d41586-021-03824-5> (2021).
- 239 2 Andrews, N. *et al.* Effectiveness of COVID-19 vaccines against the Omicron (B.1.1.529)
240 variant of concern. *medRxiv*, 2021.2012.2014.21267615, doi:10.1101/2021.12.14.21267615
241 (2021).
- 242 3 Garcia-Beltran, W. F. *et al.* mRNA-based COVID-19 vaccine boosters induce neutralizing
243 immunity against SARS-CoV-2 Omicron variant. *medRxiv*, 2021.2012.2014.21267755,
244 doi:10.1101/2021.12.14.21267755 (2021).
- 245 4 Cao, Y. *et al.* B.1.1.529 escapes the majority of SARS-CoV-2 neutralizing antibodies of diverse
246 epitopes. *bioRxiv*, 2021.2012.2007.470392, doi:10.1101/2021.12.07.470392 (2021).
- 247 5 Lu, L. *et al.* Neutralization of SARS-CoV-2 Omicron variant by sera from BNT162b2 or
248 Coronavac vaccine recipients. *medRxiv*, 2021.2012.2013.21267668,
249 doi:10.1101/2021.12.13.21267668 (2021).
- 250 6 Rössler, A., Riepler, L., Bante, D., Laer, D. v. & Kimpel, J. SARS-CoV-2 B.1.1.529 variant
251 (Omicron) evades neutralization by sera from vaccinated and convalescent individuals.
252 *medRxiv*, 2021.2012.2008.21267491, doi:10.1101/2021.12.08.21267491 (2021).
- 253 7 Planas, D. *et al.* Considerable escape of SARS-CoV-2 variant Omicron to antibody
254 neutralization. *bioRxiv*, 2021.2012.2014.472630, doi:10.1101/2021.12.14.472630 (2021).
- 255 8 Wolter, N. *et al.* Early assessment of the clinical severity of the SARS-CoV-2 Omicron variant
256 in South Africa. *medRxiv*, 2021.2012.2021.21268116, doi:10.1101/2021.12.21.21268116
257 (2021).
- 258 9 Cele, S. *et al.* Escape of SARS-CoV-2 501Y.V2 from neutralization by convalescent plasma.
259 *Nature* **593**, 142-146, doi:10.1038/s41586-021-03471-w (2021).
- 260 10 Moyo-Gwete, T. *et al.* Cross-Reactive Neutralizing Antibody Responses Elicited by SARS-CoV-
261 2 501Y.V2 (B.1.351). *N Engl J Med* **384**, 2161-2163, doi:10.1056/NEJMc2104192 (2021).
- 262 11 Greaney, A. J. *et al.* A SARS-CoV-2 variant elicits an antibody response with a shifted
263 immunodominance hierarchy. *bioRxiv*, 2021.2010.2012.464114,
264 doi:10.1101/2021.10.12.464114 (2021).
- 265 12 Cele, S. *et al.* SARS-CoV-2 evolved during advanced HIV disease immunosuppression has
266 Beta-like escape of vaccine and Delta infection elicited immunity. *medRxiv*,
267 2021.2009.2014.21263564, doi:10.1101/2021.09.14.21263564 (2021).
- 268 13 Liu, C. *et al.* The antibody response to SARS-CoV-2 Beta underscores the antigenic distance
269 to other variants. *Cell Host & Microbe* (2021).
- 270 14 Sigal, A. *et al.* Variability and memory of protein levels in human cells. *Nature* **444**, 643-646,
271 doi:10.1038/nature05316 (2006).

272

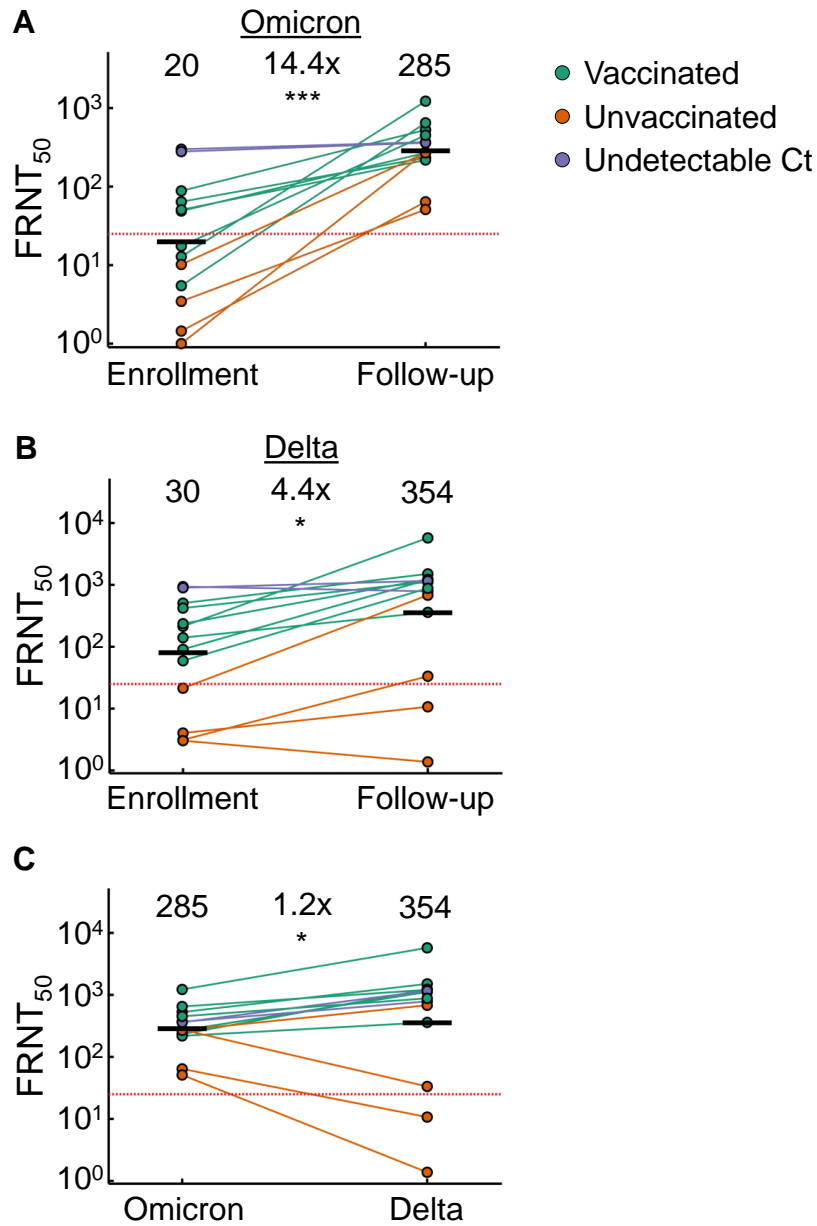


Figure 1: Enhancement of Delta neutralization by Omicron infection. (A) Omicron (A) or Delta (B) virus neutralization by blood plasma from n=13 participants infected in the Omicron infection wave at enrollment (median 4 days post-symptom onset) and at follow-up (median 14 days post-enrollment). (C) Comparison of neutralization activity against Omicron and Delta virus at follow-up. Participants were either previously vaccinated (green) or not (orange). Two participants (unvaccinated) with undetectable SARS-CoV-2 at enrollment are marked in purple. Numbers are geometric mean titers (GMT) of the reciprocal plasma dilution (FRNT₅₀) resulting in 50% reduction in the number of infection foci. Red horizontal line is most concentrated plasma used. $p=3.6 \times 10^{-4}$ for (A), $p=0.016$ for (B), and $p=0.045$ for (C) as determined by the Wilcoxon rank sum test.

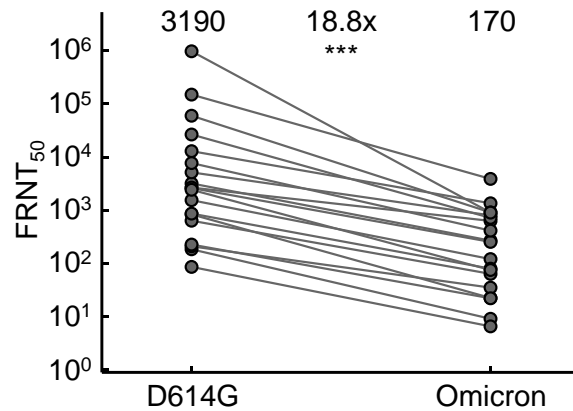


Figure S1: Neutralization of Omicron without R346K by Pfizer BNT162b2. Neutralization Omicron virus compared to D614G ancestral virus in participants vaccinated with BNT162b2. Samples were tested from n=19 participants, where n=6 were vaccinated and n=13 were vaccinated and previously infected, as described in Cele et al., Nature doi: <https://doi.org/10.1038/d41586-021-03824-5>. Numbers in black above each virus strain are GMT FRNT₅₀. Red horizontal line is most concentrated plasma used. $p=2.3 \times 10^{-4}$ by the Wilcoxon rank sum test.

Table S1: Participant details

Participant	Age	Sex	Vaccine	Symptoms date	Ct enrollment	Seq. confirmed
1	30-40	M	J&J	December	25	Yes
2	30-40	M	J&J	November	14	Yes
3	50-60	F	Pfizer	December	17	Yes
4	30-40	M	None	December	18	Yes
5	30-40	F	J&J	December	31	Yes
6	20-30	F	None	December	28	Yes
7	30-40	F	J&J	December	24	Yes
8	30-40	M	Pfizer	November	32	Yes
9	20-30	F	None	November	UND	
10	40-50	F	None	December	32	Yes
11	20-30	F	Pfizer	December	23	Yes
12	20-30	M	None	December	30	
13	20-30	F	None	December	UND	Yes

Ct: Cycle threshold by qPCR. Seq. confirmed: Verified Omicron by sequencing